Effective Connectivity within a Core Cortical Network of Face Perception: Evidence for Inferior Occipital Gyrus sensitivity for Faces with Implicit Emotion

Laura Anne Wortinger

Master's Thesis

Psychology Department
University of Oslo

May 2012

Acknowledgements

My master's thesis was part of a larger project initiated by Bruno Laeng and Tor Endestad. My assignment was completed under their excellent supervision, and I would like to thank, Tor and Bruno, sincerely for their guidance and support – you guys rock!

Abstract

Emotional face perception is a highly developed visual skill in humans that occurs along a distributed neural system including: visual, limbic, and prefrontal areas of the human brain. It has been proposed that the core regions of face perception include the inferior occipital gyrus (IOG), fusiform gyrus (FG), and superior temporal sulcus (STS). We examined the modulation of effective connectivity within these core regions during a social judgment task of affective stimuli. Emotional low spatial frequency hybrids were created, where the emotion was implicit and an apparent neutral expression was displayed, and was used in this study along with explicit expressions. Two separate event-related functional magnetic resonance imagining (*f*MRI) experiments performed on the same participants were analyzed and assessed with dynamic causal modelling (DCM) to characterize effective connectivity within core regions of face perception. We found significant modulation on both IOG to FG and STS connections for all facial conditions with the favored model being the IOG to FG connection. Additionally, we found that the emotional low spatial frequency hybrids, which were morphed with high spatial frequency neutral expressions, and neutral faces led to prominent modulation in effective connectivity from IOG to STS connection. This result suggests that the IOG is sensitive to implicit emotional faces and sorts them differently than explicit emotional faces.

Introduction

Facial expressions are an important characteristic of humans. These expressions take a multitude of forms, and therefore must require a specialized and sensitive neural system for visual perception. Two goals of visual neuroscience are to define areas and networks that makeup the human visual system and explain how its function (e.g. perceiving different emotional face stimuli) is represented in its neural correlates. Consequently, face perception seems to mediate the activation of a distributed neural system, which includes visual, limbic, and prefrontal areas of the brain. Accordingly, theories of emotional visual stimuli and face perception are expanding, as knowledge of neural networks in the brain develop.

Salient emotional face information

Expressions of happy, sad, surprise, angry, fearful, disgusted and painful faces are the most studied emotions, and extensive research is being done to identify their neural correlates in the brain. Humans have a complex and unique ability for the perception of emotional faces; however, how emotions are processed in the brain is not understood.

The standard hypothesis for processing important visual information is that emotional stimuli activate the amygdala in two ways (LeDoux, 1996; Williams et al., 2006). The low road, which can occur unconsciously, processes course visual information - but rapidly. This quick pathway is understood in terms of its evolutionary necessity. However, the high road, in conscious processing, is slower but processes fine visual information. This dual system approach is described, as having two distinct neural processes that can be activated independently from one another, but the gatekeeper, the amygdala, is responsible for sorting salient visual information to cortical areas.

In a social judgment task by Laeng et al. (2010) emotional faces were manipulated in order to tap into conscious and unconscious perception of emotional faces. Here emotional and neutral faces were separated into high and low spatial frequency (HSF and LSF) and recombined in opposite combination (emotional LSF with neutral HSF and emotional HSF

and neutral LSF). When the emotion was presented in the HSF hybrid, it was clear in the image which emotion was being expressed. However, when the emotion was presented in LSF hybrid, the emotion was not apparent in the image. Nevertheless, when researchers asked subjects to rate the image on a scale of friendliness, subjects rated the LSF emotion hybrid faces consistent with the underlying emotion, even though, the emotion was not obvious in the image. Authors concluded that when emotions are presented in LSF hybrid, unconscious processes are occurring in the brain that detects the LSF emotion in the image.

In addition, an *f*MRI study byVuilleumier, Armony, Driver, and Dolan (2003) tested face images in different spatial frequencies and found increased amygdala activation to emotional LSF faces and not neutral faces. Research is showing that the significance of emotional faces is of importance on both the conscious and unconscious level in humans.

Face perception

Face perception, possibly the most important visual information for humans, has extensive research stemming from animal studies. Single-cell recordings in face perception areas of the macaque offer valuable insight into how neurons respond to specific visual face information. Unique neuronal responses to facial expression and facial identity were found within the superior temporal sulcus and the inferior temporal gyrus, respectively (Hasselmo, Rolls, & Baylis, 1989). Additionally, cells within the STS responded specifically to different eye gaze and profile angles (D. Perrett & Mistlin, 1990; D. I. Perrett, Hietanen, Oram, & Benson, 1992). With the use of fMRI, this method offers a non-invasive means of investigating face perception regions in humans and shows similar patterns of activity, which seems to include divergent areas of the brain.

Distributed neural systems for face perception

Bruce and Young (1986) developed a functional model of face perception using studies of brain lesion patients, behavioral data in healthy individuals, and non-human primate studies, like single cell recordings and brain dissection (Hasselmo et al., 1989; D.

Perrett & Mistlin, 1990; D. I. Perrett et al., 1992). Their model suggests clear and separate processing for perception of facial identity and facial expression. However, it contains only functional information about these processes and does not address the neural correlates in the brain. It was not until 2000 that a new model was advanced of the distributed human neural systems for face perception, which identified the neural localization of these processes with *f*MRI method (Haxby, Hoffman, & Gobbini, 2000). The new model is in agreement with the functional aspects of Bruce and Young (1986), but take their idea one step further by suggesting a core region of face perception, that processes facial identity and expression separately, which works in concert with extended areas of the brain.

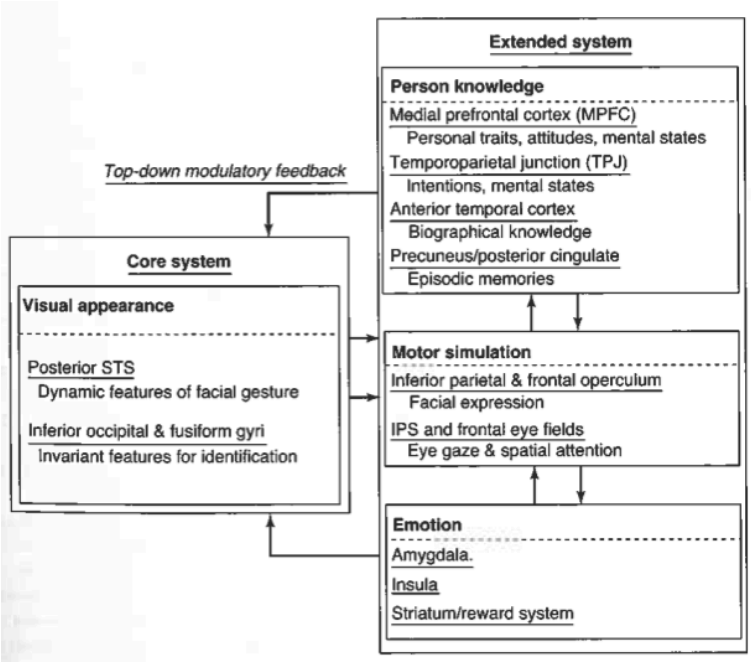

Figure 1. Updated model of distributed neural systems for face perception (Haxby & Gobbini, 2011).

The cortical neural network of face perception contains two systems (Haxby & Gobbini, 2011; Haxby et al., 2000; Haxby, Hoffman, & Gobbini, 2002). The core system for the visual analysis of faces is made up of three regions in the brain (Fig. 1). The inferior occipital gyri (IOG), the lowest visual area is responsible for early perception of facial

features. The lateral fusiform gyrus (FG) processes the invariant aspects of faces for the perception of identity. The superior temporal sulcus (STS) is activated to process changeable aspects of faces, such as eye gaze, expressions and lip movement. The extended regions are recruited to extract meaning from faces in three main ways: person knowledge, motor simulation, and emotion. Person knowledge is apparently processed by the medial prefrontal cortex (MPFC), temporoparietal junction (TPJ), anterior temporal cortex, and precuneus/ posterior cingulate. Motor simulation is processed in the inferior parietal, frontal operculum, and frontal eye fields. Finally, emotion is further processed by the amygdala, insula, and striatum. Both the core and extended systems are theorized to work together for the perception of faces in humans.

Core system. The approximate locations of the regions from the inferior occipital region are: ventral to the lateral fusiform region and dorsal to the superior temporal sulcal region. The three regions are usually identified in both the right and left hemispheres, but they tend to be more reliably activated in the right hemisphere (Haxby & Gobbini, 2011). The IOG is thought to relay information to the FG and STS, which recruits necessary areas of the extended system for processing.

Inspired by research from monkey studies, Haxby et al. (2000) found activation in the FG on tasks asking for identification of same person in subsequent photographs, whereas activation in the left STS was found for identification of same direction of eye gaze in neutral face photographs of humans. This study was the main contributor to their model of face perception. Engell and Haxby (2007) performed a similar study, but this time they used emotional faces, with direct or averted gaze, and compared results with neutral face controls. They found that direct-gaze caused an increase in activation for bilateral STS, right inferior frontal gyrus, and bilateral IOG for contrasts displaying emotion – neutral direct gaze. There were no clusters with a stronger response to neutral over emotion direct-gaze faces. However, averted-gaze emotional faces minus neutral controls revealed only greater activations in the

right STS. They concluded that the right STS region has dissociable representation for the perception of facial expression and eye gaze.

Effective connectivity research on face perception. The distributed neural systems of face perception offer an important framework in understanding the processes of face perception and have guided *f*MRI research. Lately, effective connectivity research has been adding to the knowledge of neural networks for face perception.

Effective connectivity is the measure of the flow of information among neuronal populations. This is different from functional connectivity that assesses activity correlations of neural regions, and structural connectivity that measures nerve fibers. Dynamic casual modelling (DCM) is a method for effective connectivity analysis, which creates a likely generative model of brain responses that takes into account its dynamic nature. DCM intends to reproduce a realistic neuronal model of interacting cortical regions (Friston, Harrison, & Penny, 2003). Within the Bayesian framework, DCM describes how the influences from one neuronal region cause change in another neuronal region. Specifically, it estimates connection strengths between regions and measures changes induced by experimental manipulations. Connections between regions can be assessed in one direction or bidirectionally. Effective connectivity establishes, not only if regions are working together, but also, tells us in which direction and how significant are those connections.

Fairhall and Ishai (2007) were the first to apply DCM analysis to *f*MRI data acquired during an emotional and famous face perception experiment. They found that the visual cortex processes information in a feed forward manner from the IOG to the STS and FG in both the left and right hemisphere. In fact, both emotional and famous faces modulated the connection between the IOG and FG; furthermore, the fusiform gyrus (FG) had a dominant influence on limbic and prefrontal regions. Specifically, emotional faces enhanced connection between FG and the amygdala and famous faces enhanced connection between FG and orbitofrontal cortex. Additionally, connection between amygdala and FG had a

bidirectional modulation effect (Herrington, Taylor, Grupe, Curby, & Schultz, 2011). These results illustrate a content-specific increase in connections between core and extended regions face perception.

Other investigations with effective connectivity have tested connection strengths between core and extended regions for modulation effects with emotional faces. IOG and inferior frontal gyrus (IFG) yielded significant modulation for the expression of anger, while there was less evidence for modulation from FG or amygdala to IFG (Dima, Stephan, Roiser, Friston, & Frangou, 2011). This finding is of particular interest, as it suggests affective information must be conveyed along parallel pathways, and the amygdala alone is not sufficient to transfer salient emotional information to cortical regions.

In the present study, expressions of explicit anger, implicit anger and neutral were chosen for effective connectivity analysis within the "core" regions of face perception because of the prominent research surrounding the expression of anger. Anger was highlighted in previous findings that suggest the IOG sorts this emotion differently than other negative emotions (Dima et al., 2011). In addition, most face perception research utilizes facial expressions of explicit emotions; however, implicit emotions have been shown to affect behavior with dramatic effects for implicit anger (Laeng et al., 2010). Through effective connectivity analysis, I hypothesized a stronger modulation effect for both FG and STS connections with explicit expressions of anger, than implicit anger and neutral conditions (Engell & Haxby, 2007). Second, I hypothesized an increase in modulation for explicit and implicit anger conditions between IOG-FG connection, compared to baseline neutral condition, following previous work (Fairhall & Ishai, 2007).

Method

Participants

Thirty-three college students (23 females) were recruited and compensated to participate in the study. The mean age was 23 years (SD = 4.6), and each gave written informed consent in accordance with protocols approved by Oslo University Hospital (Norway).

Material

Faces with the emotional expression of anger, fear, happy and neutral were obtained from the Karolinska Directed Emotional Faces dataset (Lundqvist, Flykt, & Öhman, 1998). Emotional faces contained 2 different presentations, broadband (BB) and low spatial frequency hybrid (LSFh), and the neutral expression was presented in only broadband, following previous work (Laeng et al., 2010). Broadband images of expressions were separated into levels of spatial frequencies. LSFh images had the emotion presentation in the low spatial frequency level only and were recombined with the neutral expression in the higher spatial frequencies. The result of the emotion LSFh is an image where the emotion is not apparent, but the neutral expression is evident (Fig. 2).

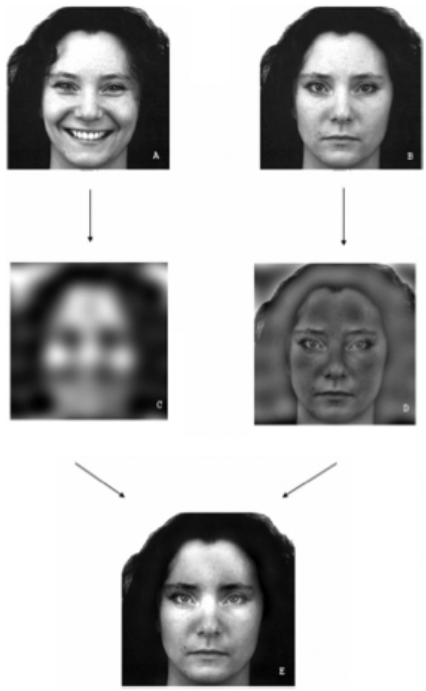

Figure 2. Broadband images of happy and neutral are separated among levels of spatial frequency (Image A & B). The low spatial frequency emotion (≤6 cycles/image) (Image C) and neutral high spatial frequency (≥7 cycles/image) (Image D) are recombined to produce a hybrid image E. The LSFh contains an emotion that is underlying, and the neutral expression is the seemingly apparent expression when viewed at the correct angle.

Design

Participants were presented with photo images, each showing one face close-up displaying either a neutral expression or one of two negative (angry or fearful) or one positive (happy) emotional expressions. They saw these faces in two separate event-related social judgment fMRI experiments conducted in a single acquisition session. In each experiment, 22 different facial identities (11 males, 11 females) were presented and lasted 16 minutes. A within-group design was utilized with two factors. Factor one contained two levels of emotional presentation, either presented in an LSFh or a broadband image. Factor two contained three emotion levels, either angry, fearful, or happy faces. Neutral faces were used to establish a baseline. Facial expressions were displayed with a randomized presentation in alternation with a fixation cross. Faces were shown for 250 milliseconds, and totaled 220 images in each session (Fig. 3). Stimuli were generated using ePrime (www.pstnet.com/eprime, version 2) and back-projected onto a mirror, mounted on the MRI head coil, by the modified F20 sx+ DLP® digital projector (Projectiondesign, Fredrikstad, Norway). Screen resolution was set at 1400×1050 pixels. Visual angle was 6˚ with a 67.5 cm distance, following previous work (Winston, Vuilleumier, & Dolan, 2003). The inter-trial interval followed a Poisson distribution with mean interval of 6.2 seconds. Participants were instructed to press one of four buttons, with their dominant hand, on a MRI compatible response box indicating the degree of friendliness each image contained. Button press, with one of the 4 fingers, indicated unfriendly, somewhat unfriendly, somewhat friendly, or friendly. Response times and friendliness ratings were collected by use of ePrime software.

For simplicity, emotion LSFh will be referred to as implicit condition, as the emotion is not apparent in the image. Emotion BB will be referred to as explicit condition, as the emotion is apparent in the image.

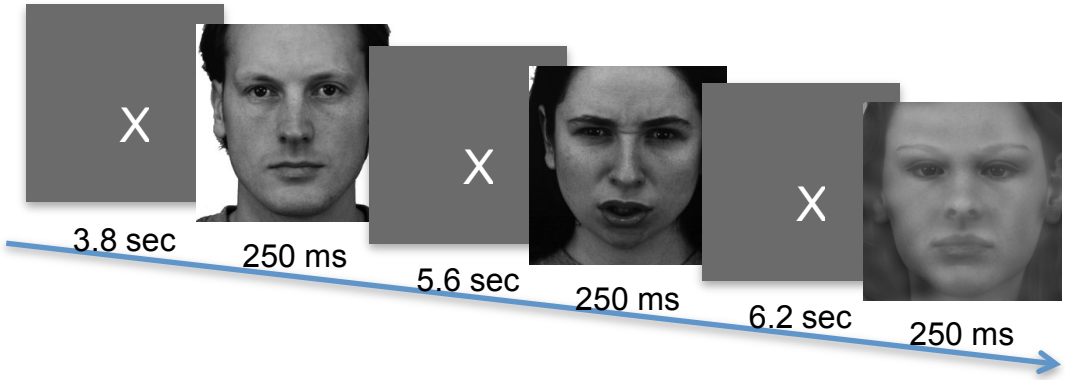

Figure 3. Illustration of a series of trials that probed social impressions about faces. Participants viewed faces of either: neutral BB, emotion BB or emotion LSFh conditions. During each of the two experiments, participants judged the degree of friendliness of each face by pressing one of four keys on an MRI compatible response box.

Image acquisition

Gradient echo (GRE) planar MR images were acquired using a 3.0 T Philips MR system fitted with 40 mT/m high-speed gradients. Foam padding was used to limit head motion, and a quadrature birdcage head coil was used for radio frequency transmission and reception. In each of the 34 noncontiguous planes, parallel to the intercommissural (AC-PC) plane, 15 degrees was added to the anterior-posterior (RL degree field). Slices at this angle are congruent with the anatomical orientation of the amygdala, a region of interest, for later studies. T2* - weighted MR images reporting BOLD contrast were acquired with time repetition (TR) = 2000 ms, time echo (TE) = 30 ms, flip angle = 80°, slice thickness = 3 mm, slice gap = 0 mm, matrix size = 80 x 80, and voxel dimensions = 3 x 3 x 3. Functional images acquired for each participant was 2 x 480.

During the same session, high-resolution T1 weighted structural images were acquired with TR = 6.7 ms, TE = 3.1 ms, TI = 830 ms, flip angle = 8°, slice thickness = 1.2 mm, matrix size = 256 x 213, FOV = 256 x 204 mm, voxel dimensions = 1 x 1 x 1.5 mm, and number of signal averages (NSA) = 1 for subsequent co-registration.

Image processing

Image preprocessing and GLM analysis was completed with SPM8 software package (Wellcome Trust Centre for Neuroimaging, London, UK; http://www.fil.ion.ucl.ac.uk); DCM8 was used for effective connectivity analysis.

Preprocessing. The fast and efficient echo planar imagining (EPI) sequences, a variant of GRE and most common method in functional MRI acquisition, were corrected for spatial and intensity distortions caused by magnetic susceptibility variations. We applied a nonlinear registration procedure, following previous work (Holland, Kuperman, & Dale, 2010). As accurate and clear images are essential for analysis, the correction algorithm was important, in particular, for small structures, which are prone to signal loss due to distortions. The corrected functional EPI images were then realigned to correct for movement. Participants over 3 mm of movement in any direction were removed from further analysis. Structural images were co-registered with functional images and segmented to produce spatial normalization parameters (template for the parameters was provided by the Montreal Neurological Institute (MNI)). The produced parameters were then used to normalize the functional images. Finally, the spatially normalized images were smoothed with an 8 mm full-width half-maximum Gaussian kernel, as per (Ashburner, Chen, Moran, Glauche, & Phillips, 2010).

First level (within-subject) analysis. Data from the two sessions were concatenated and modeled with a general linear model (Ashburner et al., 2010). A canonical hemodynamic response function was convolved with vectors of onset times representing each condition. Two regressors were created, one representing all faces, which included anger BB, anger LSFh, and neutral, and one representing each condition separately. Time series correlations, low-frequency noise, and systematic differences across trials were removed using a 128 s high-pass filter. Nuisance covariates were accounted for with six movement parameters.

Second level (between-subject) analysis. Group-level analysis was performed using a one-way ANOVA of single-subject contrast images (Ashburner et al., 2010). A statistic

summary of the main effect of all faces was assessed to identify group maxima in regions of interest. Coordinates for inferior occipital gyrus (IOG), fusiform gyrus (FG) and superior temporal sulcus (STS) were produced with a statistical threshold adjusted to FWE of $p = 0.05$ and corrected for multiple comparisons across whole brain.

Volumes of interest

Following previous work, Fairhall and Ishai (2007), a priori volumes of interest (VOIs) were selected within the core network involved in face processing. With an anatomical mask created in PickAtlas toolbox (Maldjian, Laurienti, Kraft, & Burdette, 2003), we defined group maximums, within each region of interest. A 4 mm sphere mask, centered around group maxima, was created and used in individual SPM to chose subject-specific maxima within the same anatomical area. Regional time series were summarized with the first eigenvariate of all activated ($p < 0.05$) voxels within 5 mm of the subject-specific maxima. The VOIs are reported in MNI coordinate system and contained the inferior occipital gyrus (IOG) (-42, -82, -11), the fusiform gyrus (FG) (-39, -61, -20), and the superior temporal sulcus (STS) (-48, -46, 7).

Dynamic causal modelling

Dynamic causal modelling (DCM) characterizes effective connectivity by measuring information flow in direction and strength on connections between neuronal populations (Friston et al., 2003). It is not just an analysis of regional correlations; its aim is to measure strength of intrinsic synaptic connections and modulations caused by experimental manipulation. In this study, the parameters of the model were theoretically based on the core regions of face perception (Haxby et al., 2000, 2002) and the directionality of connection parameters was experimentally established by Fairhall and Ishai (2007). Accordingly, a three-area model was specified for all subjects with forward connections between IOG to FG and STS. The main effect of "all faces" was used as the driving input into the IOG, the lowest

visual area. From the base model, modulation effects on these connections were systematically manipulated and produced three alternative model variants (Fig. 4).

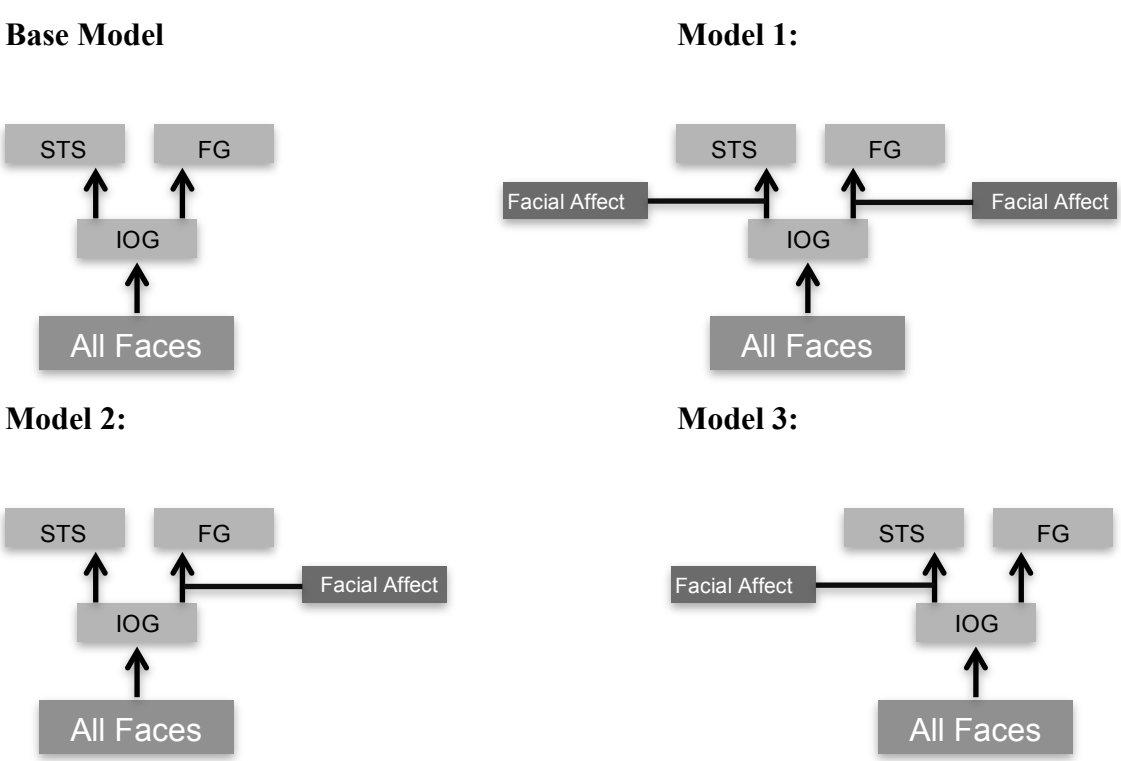

Figure 4. Model specification. A three-area DCM was specified with forward endogenous connections between IOG, FG and STS. Facial affect corresponds to the conditions of the experiment either explicit angry, implicit angry or neutral. "All faces" is the driving input into the IOG and model.

As stated in the Introduction, the primary goal of this study was to assess the modulation effects of explicit angry, implicit angry, and neutral face conditions on connections between the IOG to the FG and STS. These conditions are of particular interest for this study and effective connectivity analyses are restricted to these conditions. Accordingly, explicit anger yielded an alternate route of processing from the IOG in previous work (Dima et al., 2011). In addition, implicit anger was rated least friendly among implicit emotion conditions in a social judgment task (Laeng et al., 2010). Neutral expression was

used to establish a baseline for activations. Each condition alone was used to test for differences in context-specific interactions on these connections.

Model comparison. The nature of the model space can be defined by making inferences on the model structure and model parameters. As model parameters were already established, the goal of this study was to make inferences on model structure from context-specific modulation of connectivity between these regions. There was an assumption that the optimal model structure would be identical across participants. Therefore, model comparison was carried out using Bayesian model selection (BMS) with a fixed-effects (FFX) inference analysis.

BMS compares the ability of the model evidence to explain the data. Specifically, the Bayesian framework addresses the probability of the data from the *i*th subjects data given the *j*th model: $p(yi/mj)$. A Bayes factor is computed by two criteria: the Bayesian information criterion (BIC) and the Akaike's information criterion (AIC) (Penny, Stephan, Mechelli, & Friston, 2004). Furthermore, consistent evidence in favor of a model should be considered if both AIC and BIC provide a Bayes factor of at least the natural exponent e = 2.7183, and a Bayes factor of 3-20 provides positive evidence in favor of the model (Raftery, 1995). In addition, BMS gives the model posterior probability, which explains how well the data is generated by the model (Stephan, Penny, Daunizeau, Moran, & Friston, 2009). The log evidence and the posterior probability together represent the likelihood that the data fits the model.

Connectivity strength. When a DCM is created, it estimates connectivity parameters for three main matrices. Matrix A represents the intrinsic or endogenous connectivity between the regions, which does not contain any experimental manipulations. Matrix B holds the change in coupling among the regions and shows the modulation of effective connectivity by experimental manipulations. Finally, matrix C contains the extrinsic influences of input on neuronal activity (Friston et al., 2003). In addition to the estimation parameters of the actual

connectivity, the probability of these estimates is also generated for each of the matrices. In this study, the connectivity estimates for each of the matrices was tested for consistency using the Kolmogorov-Smirnov test for all participants and models. The Kolmogorov-Smirnov test was used because our dataset did not follow a normal distribution. The modulation means were approximately balanced around zero; they contained both positive and negative numbers, which zeroed each other out. Standard t-tests do not see the differences in such datasets, and therefore the Kolmogorov-Smirnov test was implemented.

The Bayesian Model Averaging (BMA) feature calculates the average connectivity estimates, weighted by their posterior model probability, across all models and all subjects (Penny et al., 2010). The results, from fixed effects BMA, produce a corrected mean in connectivity strengths across all parameters of the model.

Statistical Analyses

A repeated measures analysis of variance (ANOVA) and paired samples t-tests were performed on response times (RTs) and friendliness ratings using SPSS 19.

Results

Behavioral analysis was carried out on neutral and both presentations of angry, fearful and happy faces.

Behavioral data

Response times. We performed a 2 (emotional presentation: explicit, implicit) x 3 (emotion: anger, fear, happy) repeated-measures analysis of variance (ANOVA) on response times (RTs). There was a strong main effect of emotional presentation, $F(1, 32) = 25.060$, $p < .0001$, $\eta^2 = .432$, as well as a strong main effect of emotion, $F(1, 32) = 48.383$, $p < .0001$, $\eta^2 = .595$. Together, there was a strong interaction effect with both emotional presentation and emotion, $F(1, 32) = 13.502$, $p < .0001$, $\eta^2 = .290$. RTs across emotional presentation and

emotions are illustrated in figure 5. Three paired samples t-tests were used to compare emotional presentation and six paired samples t-tests were used to compare emotions.

Emotional presentation comparisons for RTs found anger, as explicit and implicit conditions, to be significantly different (M -63.2, SD 87.8), $t(32) = -4.20$, $p < .0001$. However, expression of fear, as either explicit or implicit conditions, was not significantly different (M -8.3, SD 109.0), $t(32) = -0.45$, $p = .659$. Expression of happy, in either explicit and implicit conditions, was significantly different (M -113.4, SD 99.1), $t(32) = -6.68$, $p < .0001$. Comparing RTs between emotions and within each presentation, found emotions to be significantly different among themselves with a $p < .001$ or less for all emotions, except comparison of implicit anger and implicit happy. Implicit anger and happy were not significantly different from each other (M 13.8, SD 54.1), $t(32) = 1.49$, $p = .145$. Our results suggest that, when responding to fear, implicit or explicit, participants did not significantly differ in their RTs. Additionally, implicit anger and happy conditions did not yield any significant difference in response time.

Explicit neutral. A comparison of means was performed for the explicit neutral condition against all six emotion presentations and was not significantly different from explicit fear (M -12.15, SD 104.33), t(32) = -.679, p = .502 and implicit anger (M 14.40, SD 63.61), t(32) = 1.32, p = .196. We applied Bonferroni corrections for multiple comparisons, resulting in an adjusted threshold of alpha = 0.0083. After adjusting for Bonferroni, our results also found no differences for implicit fear (M -20.45, SD 56.51), t(32) = -2.11, p = .042.

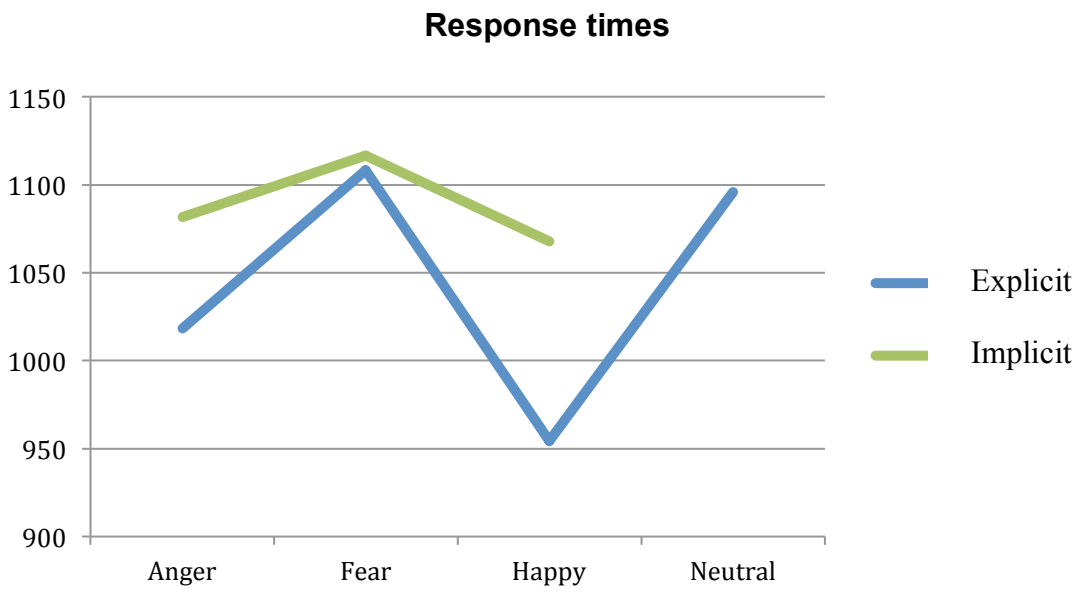

Figure 5. RTs across emotions: anger, fear, happy and neutral for explicit and implicit conditions.

Friendliness ratings. We performed a 2 (emotional presentation: explicit, implicit) x 3 (emotion: anger, fear, happy) repeated-measures analysis of variance (ANOVA) on friendliness ratings. There was a strong main effect of emotion, $F(1, 32) = 581.615$, $p < .0001$, $\eta^2 = .946$. Interestingly, there was a strong interaction effect of emotional presentation and emotion combined, $F(1, 32) = 315.341$, $p < .0001$, $\eta^2 = .905$. Friendliness ratings across emotional presentations and emotions are illustrated in figure 6. Three paired samples t-tests were used to compare emotional presentation and six paired samples t-tests were used to compare emotions. All tests were significantly different with a $p < .0001$ or less. Our results show significantly different ratings for emotions, within and between, emotional presentations. Specifically, implicit rating trends correspond with the degree of friendliness of explicit ones, where anger being significantly rated as more unfriendly than happy.

Explicit neutral. Paired samples t-tests was used to compare means of explicit neutral against all six emotion presentations and found significant differences in all emotions except implicit fear (M -.037, SD .121), t(32) = -1.77, p = .086. We applied Bonferroni corrections

for multiple comparisons, resulting in an adjusted threshold of alpha = 0.0083. Again, our values showed a significant difference for all emotions except implicit fear.

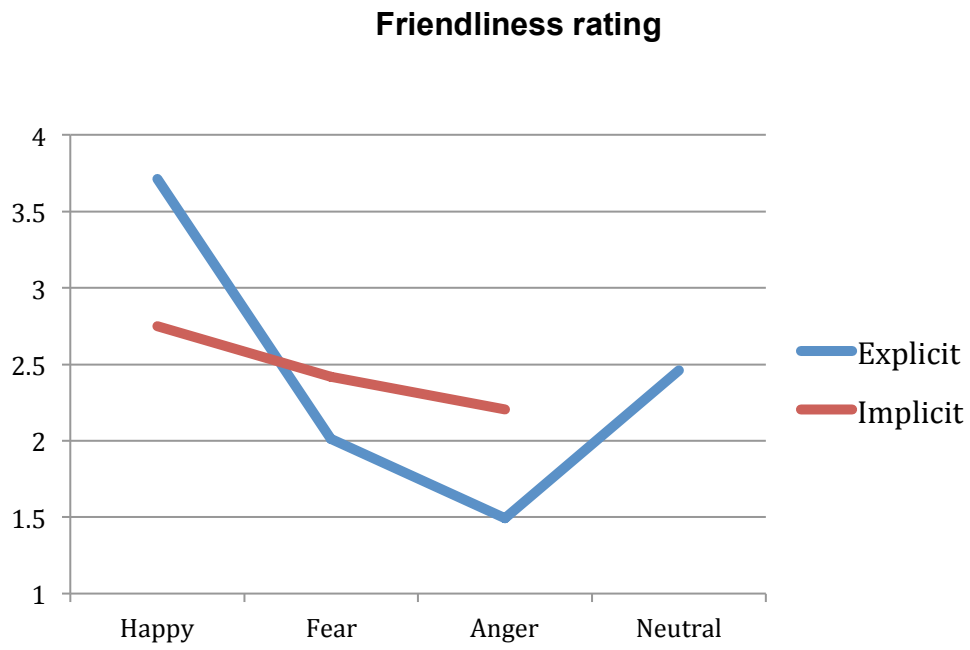

Figure 6. Friendliness ratings across emotions: happy, fear, anger and neutral explicit and happy, fear, and anger implicit conditions. Both emotional presentations show the same trend in ratings where anger is, specifically, less friendly than happy.

fMRI results

Robust activations in response to all faces were apparent in visual, temporal and prefrontal areas (Dima et al., 2011; Fairhall & Ishai, 2007; Vytal & Hamann, 2010) (Fig. 7 and Table 1). In accordance with previous work, we found consistent and strong activations in the particular areas of interest of this study, IOG, FG, STS.

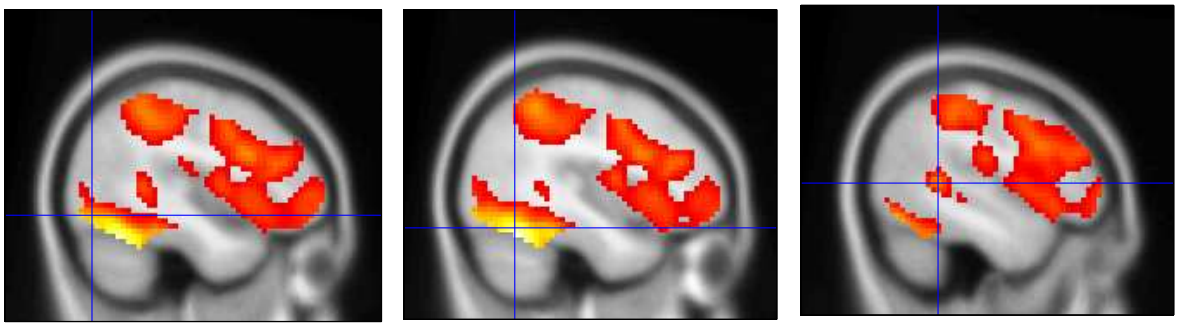

Figure 7. Whole brain image activations showing the 3 core regions of face perception. "All Faces" regressor displayed - IOG, FG and STS corrected for FWE, $p < .05$.

Table 1. Voxel-based whole brain SPM analysis listing regions having a significant main effects in terms of hemodynamic responses to the presentation of all faces.

Brain Region	BA	Laterality	Coordinates *x*	*y*	*z*	Cluster size (voxels)	*Z*-value
Fusiform gyrus	37	L	-39	-61	-20	2950	7.59
Inferior occipital gyrus	N\A	L	-42	-82	-11		5.90
Lingual gyrus	N\A	R	9	-88	-2		7.59
Lingual gyrus	N\A	L	-6	-85	-5		7.26
Precuneus	7	L	-24	-52	43	269	6.53
Middle frontal gyrus	N\A	R	51	29	25	98	5.79
Superior Parietal Lobule	7	R	30	-61	49	70	5.37
Insula		R	33	23	1	21	5.15
		L	-42	11	25	26	5.00
Middle temporal gyrus	N\A	L	-48	-46	4	5	4.98
Superior temporal gyrus	N\A	L	-48	-46	7		6.19
Extra-Nuclear	N\A	L	-21	-25	-5	2	4.73
Thalamus	N\A	L	-12	-10	-2	3	4.66
Inferior frontal gyrus	N\A	L	-33	20	-2	1	4.60
Insula		L	-30	26	1	1	4.59

Connectivity results

Comparing neutral models. Model 2 (IOG-FG) and Model 3 (IOG-STS) provided Bayes factors greater than 3, which mean there is positive evidence in favor of model 2 and 3 (Fig. 6). The posterior probability yielded Model 2 as the generator of the data at 99%, which infers the IOG to FG connection is the dominant pathway in the flow of information for the data. There is positive evidence that neutral faces are increasing both connection strengths; however, after weighting all the parameters, Model 2 seems to be the favored route of the data.

Comparing implicit anger emotion models. Model 2 (IOG-FG) and Model 3 (IOG-STS) provided Bayes factors greater than 3, which mean there is positive evidence in favor of model 2 and 3 (Fig. 6). The posterior probability yielded Model 2 as the generator of the data at 100%, which infers the IOG to FG connection is the dominant pathway in the flow of information for the data. There is positive evidence that implicit angry faces are increasing both connection strengths; however, after weighting all the parameters, Model 2 seems to be the favored route of the data.

Comparing explicit anger emotion models. Only Model 2 (IOG-FG) provided Bayes factors greater than 3, which mean there is positive evidence in favor of model 2 (Fig. 8). The posterior probability yielded Model 2 as the generator of the data at 100%, which infers the IOG to FG connection is the dominant pathway in the flow of information for the data.

Figure 8. Bayes Factor and posterior probabilities for the 3 models specified in each condition (N = 15). Model 2 is the favored model for neutral, implicit anger and explicit anger conditions. Interestingly, positive evidence in favor of Model 2 and Model 3 for neutral and implicit anger conditions.

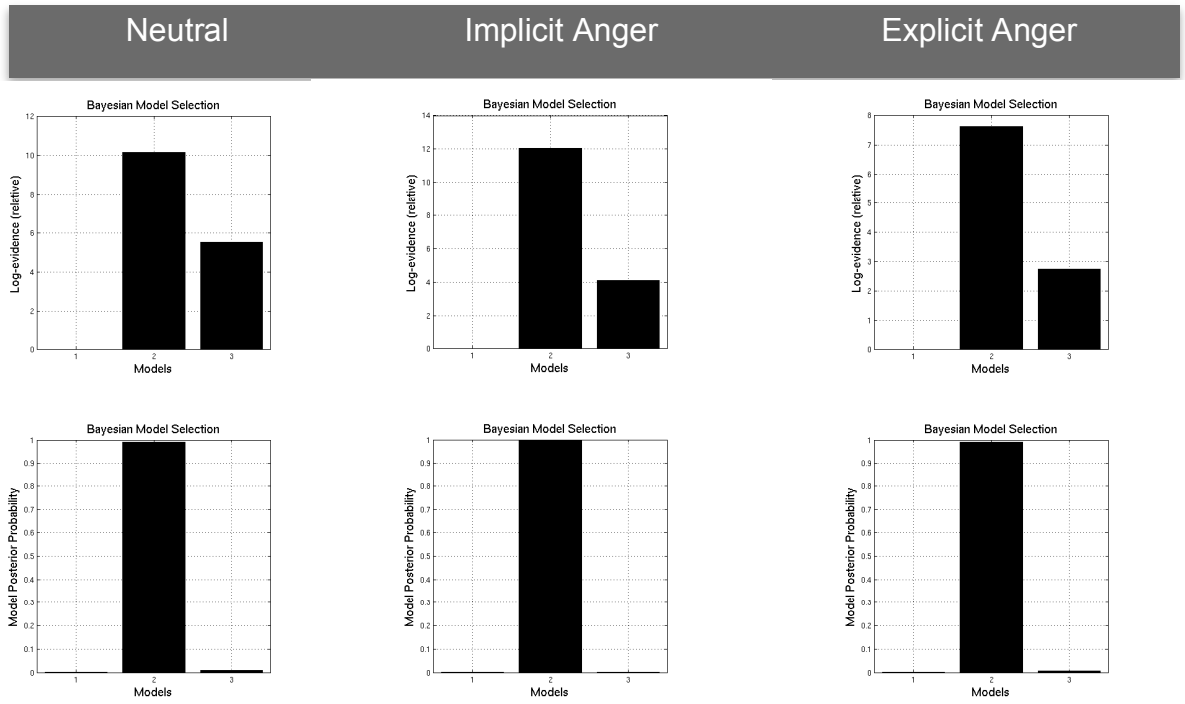

Strength of effective connectivity. The actual intrinsic connection strengths were significantly established between the regions with *p* values < 0.0001. This means that without any experimental manipulations the IOG, FG and STS are highly connected. The coupling strength between both regions yielded significant increase in connectivity for all experimental conditions, but only modulation of IOG-STS connection for implicit anger and neutral survived Bonferroni corrections for multiple comparisons (Table 2). The modulation of the IOG-STS connection was highly significant for implicit anger and neutral and will be explained further in the discussion. Fixed effects BMA analysis was used to obtain connection averages weighted by their posterior model probabilities (Table 3).

Table 2. DCM intrinsic, input, and modulation estimates for all actual connections and regions across all subjects and models.

Effective connectivity parameters	Mean	Min	Max	SD	*p* value	
Intrinsic connectivity						
IOG - FG	1.2477	0.4240	2.3981	0.4583	<0.0001	**
IOG - STS	0.3269	0.0902	0.7168	0.1337	<0.0001	**
Extrinsic input						
IOG	0.5168	0.1339	1.0250	0.2324	<0.0001	**
Modulation of connectivity						
IOG - FG, neutral	0.1307	-0.7679	1.0087	0.3740	0.0033	*
IOG, STS, neutral	-0.0446	-0.6778	0.6438	0.3096	0.0013	**
IOG - FG, implicit anger	0.1176	-0.6037	0.6127	0.3158	0.0037	*
IOG - STS, implicit anger	0.0875	-0.2199	0.4291	0.1761	<0.0001	**
IOG - FG, explicit anger	0.0701	-0.6631	1.0421	0.4207	0.0216	*
IOG - STS, explicit anger	0.1240	-0.7068	0.9119	0.4561	0.0366	*

*Difference significant at $p < 0.05$, uncorrected for multiple comparisons.

**Difference survives Bonferroni corrections for multiple comparisons, corrected at $p = 0.002$.

Table 3. BMA for intrinsic, input and modulation on all connections and regions across all subjects and models. BMA uses the parameter estimates, weighted by their posterior model probability, and calculates a true mean for each parameter.

Effective connectivity parameters	Mean	SD
Intrinsic connectivity		
IOG - FG	1.2783	0.0999
IOG - STS	0.3455	0.0478
Extrinsic input		
IOG	0.4861	0.0284
Modulation of connectivity		
IOG - FG, neutral	0.1385	0.1463
IOG - FG, implicit anger	0.1183	0.1450
IOG - FG, explicit anger	0.0811	0.1465

The results of the DCM analyses are summarized in Figure 9 and show the IOG-FG connection as the favored pathway for neutral, implicit anger, and explicit anger face stimuli. However, the IOG seems to be modulating information from neutral and implicit anger conditions with significant increase in coupling strength. This finding suggests the IOG seems to be sorting relevant information along both routes.

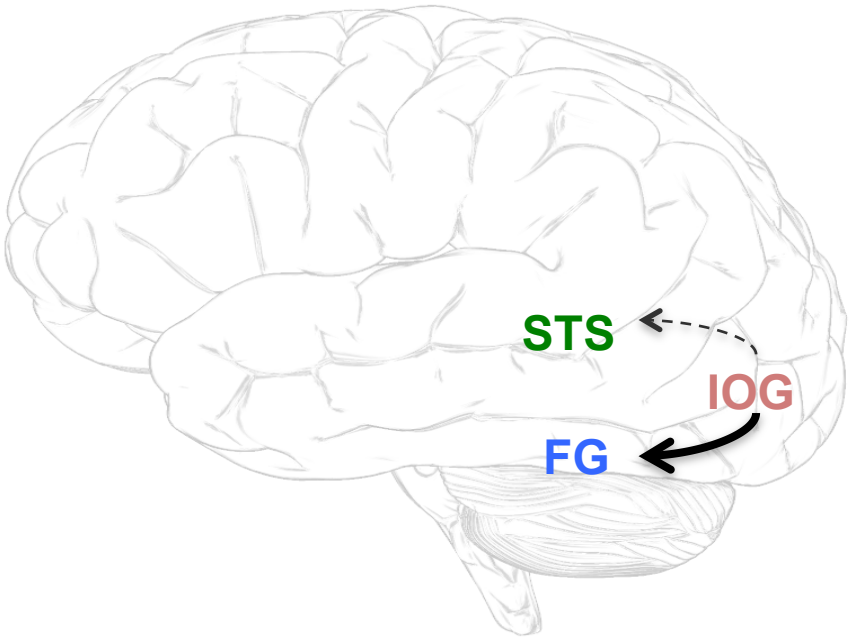

Figure 9. Arrows indicate significant endogenous connections between the regions ($p < 0.0001$). Thick black arrow indicates endogenous connections significantly modulated by neutral, implicit anger, and explicit face conditions and favored pathway generating the data. Dashed arrow represents highly significant modulation on connection for implicit anger and neutral face conditions.

Discussion

The present findings failed to support the hypothesis for a stronger modulation effect for both FG and STS connections with the explicit expression of anger, than implicit and neutral conditions. Instead, the present study yielded a significant main effect for all types of face stimuli (explicit anger, implicit anger, neutral) with primary activation of "core" regions in the left hemisphere. This study implemented a regressor with two-thirds of the variance containing non-expression faces and one-third with an explicit expression of anger. However, emotional face perception research shows the right hemisphere to be dominating in processing emotions (Dima et al., 2011; Engell & Haxby, 2007; Fairhall & Ishai, 2007; Haxby et al., 2002; Herrington et al., 2011; Vuilleumier et al., 2003). Nevertheless, emotionless faces have been reported to significantly activate the left side (Haxby et al., 2000). I reported significant modulation effects for all conditions, on left hemisphere

connections, with the favored pathway being the IOG to FG (Fig. 8). However, implicit anger and neutral expressions significantly increased connectivity strength in the IOG to STS pathway (Table 2). In addition, this study found response times for implicit anger and neutral to be similar (Figure 5), but there was a significant difference in friendliness rating where implicit anger was rated less friendly than neutral (Figure 6). Since implicit anger and neutral faces are the unapparent emotion conditions driving the variance of the model, my explanation will be focused on discussing what is underlying in this social judgment paradigm.

From single cell recordings in face perception areas of the macaque brain, researchers identified cells sensitive to identity and eye gaze (Hasselmo et al., 1989; D. Perrett & Mistlin, 1990; D. I. Perrett et al., 1992). These findings inspired researchers to find homologous areas in humans, manipulating conditions in *f*MRI experiments. Still and dynamic images of facial expressions with variety of poses and eye positions have been used to better understand the physiology of the regions. A theory was advanced to interpret these findings wherein the IOG is a region for feature perception that forwards information to the FG for invariant feature perception of identity and STS for changeable feature perception of expression (Haxby & Gobbini, 2011; Haxby et al., 2000, 2002). Robust, bilateral activations for IOG, FG, and STS have been reported, and processing between regions has been found to occur in a feed forward direction from the IOG to the FG and STS (Fairhall & Ishai, 2007).

Lately research has discovered that the role of "core" regions is not so simple. The IOG seems to be more sensitive to both identity and expression perception than once thought. Using TMS (transcranial magnetic stimulation), a device that temporally inhibits neural excitation in a specific area, it was found that the right orbital face area (OFA-located within IOG) was involved in the discrimination of differences in individual features of a face (Pitcher, Walsh, Yovel, & Duchaine, 2007). In addition another study found repetitive TMS applied over the right OFA disrupted the ability of observers to match faces with

corresponding emotional expression (Pitcher, Garrido, Walsh, & Duchaine, 2008). In fact the IOG was found to discriminate between the expressions of anger and other negative expressions, with an increase in modulation to the inferior frontal gyrus (Dima et al., 2011). Furthermore Li et al. (2010) findings support a model, through DCM connectivity analysis, where the orbitofrontal cortex (OFC) seems to exert top-down regulation of the OFA, which detects illusory face features and increases coupling to FG. The role of IOG seems to be interactive with frontal regions, which further facilitates face perception, and exclusive hierarchical feed-forward analogies are not true representation of activities (Atkinson & Adolphs, 2011). In the present study, the IOG seems to increase connectivity to STS region for the expression of implicit anger and neutral, which is different from the explicit anger condition. One implication may be that the IOG is sensitive to facial uncertainty that might require further assessment from STS.

Accordingly the role of the STS does not seem to be straightforward. Still photos activate STS and researchers rationalize that this response "may reflect involvement in the perception of potential movement or the evaluation of changeable aspects of a face that can vary with movement" (Haxby et al., 2002, p. 61). However, a social judgment task found the intentional engagement of the STS, where the left STS was significantly activated in the untrustworthy conditions (Winston, Strange, O'Doherty, & Dolan, 2001). A TMS study found trustworthiness judgments were significantly impaired when delivered over left and right STS, but not when it was delivered over right OFA (Dzhelyova, Ellison, & Atkinson, 2011). Another study used dynamic images and concluded bilateral STS activation seems to be involved in the general changing of social signals (Puce & Perrett, 2003). An audio/visual task that combines stimuli found different functions for left and right STS, where left STS seems to be activated for the integration of speech and right STS for the integration of emotion (Calvert, Hansen, Iversen, & Brammer, 2001). In these examples the role of STS seems to be involved in extracting meaning from visual stimuli and less with the basic

function of spatial attention and emotion expression. Haxby and Gobbini (2011) now explain, "The variable response of the pSTS maybe due to the ambiguous meaning of direct and averted eye gaze," (p. 103). A direct eye gaze could be a sign of interest or threat, and an averted eye gaze could be to signal attention or mean lack of interest. The involvement of STS activity within face perception seems to be evolving. In this study the significant modulation effect to the left STS could correspond with the intentional engagement of STS in the social judgment task for further evaluation of implicit anger and neutral expressions.

The fusiform gyrus responds more to emotional faces with direct gaze, and face response in FG seems to be strongly modulated by attention (Engell & Haxby, 2007; Furey et al., 2006; Wojciulik, Kanwisher, & Driver, 1998). The current study found explicit anger, implicit anger, and neutral expressions significantly increased coupling between IOG and FG. The ventral pathway seems to be the generator of the data (Fig. 8); even though, there was significant activation in the dorsal, IOG to STS connection. This finding was explained by W. Penny, founder and expert behind DCM and BMA (personal communication, April 18, 2012):

The significant modulation of the IOG-STS pathway is not inconsistent with the fact that model 2 (IOG-FG) provides a better explanation of the data than either models 1 or 3. If c is a connection then the posterior probability of it under model m is p(c|m,y) where y is the data and can also compute the posterior probability of the model, p(m|y). BMA then computes the posterior probability of the connections by integrating out model uncertainty (ie averaging over models): p(c|y) = sum_i p(c|m=i,y) p(m=i|y). It will average over all models but weighted by p(m|y), so if p(m=2|y) is much bigger than p(m=1|y) and p(m=3|y) then the values from model 2 will dominate.

The IOG connection to FG was strongly modulated by all conditions. However, our second hypothesis that explicit and implicit anger expressions would produce stronger modulation effects between IOG to FG, over neutral conditions, was not supported by the

findings of this study (Table 2). Even though the intrinsic connection between IOG and FG was stronger than IOG to STS, the fact that explicit and implicit emotions did not produce the greatest effects across conditions may be an issue of laterality and should be investigated with future studies.

Nevertheless, Turk-Browne, Norman-Haignere, and McCarthy (2010) developed a new partial functional connectivity method which confirmed that the FG–pSTS resting correlations were face-specific. Specifically they found category-specific interactions, without visual input, which implies resting state may provide an underlying basis for task processing. The "core" regions are reported as having highly significant intrinsic connections between regions (Dima et al., 2011; Fairhall & Ishai, 2007), similar to this study (Table 2). Together with specificity of resting state data, it seems these areas are highly specialized in working to extract meaning from faces.

It is possible that the emotion low spatial frequency hybrid activates two different processes in the brain – face perception and conflict resolution. The implicit emotion may be prompting a system, such as the conflict resolution process often explained in Stroop tasks (Egner, 2011). However, unlike classic Stroop tasks where both variables are explicit, the emotion LSF hybrid has only one factor (neutral face) explicitly displayed and the other, the emotion, is underlying or unconscious. The increase in response time for the emotion LSFh could be similar to the classic decline in performance due to conflict effect (Stroop effect). Furthermore the modulation increase to the STS for the emotion LSFh could represent the activation of cognitive resources needed to resolve conflicting stimulus information within face perception. Again, future directions for analysis could investigate how emotion LSFh is processed, including extended brain regions, to resolve inter-stimulus conflict, as our results showed anger LSFh were rated in accordance with the underlying emotion (Fig. 6).

This study followed protocols put forth by previous DCM analysis for face perception (Dima et al., 2011; Fairhall & Ishai, 2007). A major limitation to their method is the strict

criteria for volume of interest (VOI) extractions. If a participant does not have significant activations, within 4mm of the group maxima, for all regions of interest, the participant is excluded. This study excluded 10 participants due to no activation and found STS to be the main problem. Fairhall and Ishai (2007) conclude that regional differences between subjects are likely subject specific variations in signal-to-noise ratio than variations in structures. Future DCM studies may overcome these limitations by employing a functional localizer to extract subject specific coordinates for VOI extraction, which would enable the identification of all regions in all participants.

In the present study, there was a significant main effect for all face stimuli with primary activation of core regions in the left hemisphere. The core regions also contained highly significant intrinsic connections. Additionally there were significant modulation effects for all face conditions on both connections, with the favored pathway being the IOG to FG. However, results showed that the IOG was sensitive to implicit expressions and sorted this information differently than the explicit facial expression. The reaction time for explicit anger was faster than both implicit anger and neutral conditions, which were not significantly different from each other. However, implicit and explicit angry faces were rated significantly less friendly than neutral faces. This study provides an opening to future studies to investigation into the role of the right and left STS in implicit and explicit emotion processing within face perception areas of the brain. These studies should include the frontal regions and amygdala to gain insight on laterality and conflict resolution processes of salient emotion and seemingly emotionless face stimuli to better understand their neural correlates within face perception.

References

Ashburner, J., Chen, C.-c., Moran, R., Henson, R., , Glauche, V., & Phillips, C. (2010). SPM8 Manual The FIL Methods Group *Imaging, 43*(3).

Atkinson, A. P., & Adolphs, R. (2011). The neuropsychology of face perception: beyond simple dissociations and functional selectivity. [Review]. *Philos Trans R Soc Lond B Biol Sci, 366*(1571), 1726-1738. doi: 10.1098/rstb.2010.0349

Bruce, V., & Young, A. (1986). Understanding Face Recognition. *British Journal of Psychology, 77*, 305-327.

Calvert, G. A., Hansen, P. C., Iversen, S. D., & Brammer, M. J. (2001). Detection of audio-visual integration sites in humans by application of electrophysiological criteria to the BOLD effect. [Research Support, Non-U.S. Gov't]. *Neuroimage, 14*(2), 427-438. doi: 10.1006/nimg.2001.0812

Dima, D., Stephan, K. E., Roiser, J. P., Friston, K. J., & Frangou, S. (2011). Effective connectivity during processing of facial affect: evidence for multiple parallel pathways. [Comparative Study Research Support, Non-U.S. Gov't]. *J Neurosci, 31*(40), 14378-14385. doi: 10.1523/JNEUROSCI.2400-11.2011

Dzhelyova, M. P., Ellison, A., & Atkinson, A. P. (2011). Event-related repetitive TMS reveals distinct, critical roles for right OFA and bilateral posterior STS in judging the sex and trustworthiness of faces. *J Cogn Neurosci, 23*(10), 2782-2796. doi: 10.1162/jocn.2011.21604

Egner, T. (2011). Right ventrolateral prefrontal cortex mediates individual differences in conflict-driven cognitive control. [Research Support, N.I.H., Extramural]. *J Cogn Neurosci, 23*(12), 3903-3913. doi: 10.1162/jocn_a_00064

Engell, A. D., & Haxby, J. V. (2007). Facial expression and gaze-direction in human superior temporal sulcus. *Neuropsychologia, 45*(14), 3234-3241. doi: Doi 10.1016/J.Neuropsychologia.2007.06.022

Fairhall, S. L., & Ishai, A. (2007). Effective connectivity within the distributed cortical network for face perception. *Cerebral Cortex, 17*(10), 2400-2406. doi: Doi 10.1093/Cercor/Bhl148

Friston, K. J., Harrison, L., & Penny, W. (2003). Dynamic causal modelling. [Research Support, Non-U.S. Gov't]. *Neuroimage, 19*(4), 1273-1302.

Furey, M. L., Tanskanen, T., Beauchamp, M. S., Avikainen, S., Uutela, K., Hari, R., & Haxby, J. V. (2006). Dissociation of face-selective cortical responses by attention. *Proc Natl Acad Sci U S A, 103*(4), 1065-1070. doi: 10.1073/pnas.0510124103

Hasselmo, M. E., Rolls, E. T., & Baylis, G. C. (1989). The role of expression and identity in the face-selective responses of neurons in the temporal visual cortex of the monkey. [Research Support, Non-U.S. Gov't]. *Behav Brain Res, 32*(3), 203-218.

Haxby, J. V., & Gobbini, M. I. (2011). Distributed neural systems for face perception. In A. J. Calder, G. Rhodes, M. H. Johnson & J. V. Haxby (Eds.), *The Oxford Handbook of Face Perception* (pp. 94-110). Oxford: Oxford University Press.

Haxby, J. V., Hoffman, E. A., & Gobbini, M. I. (2000). The distributed human neural system for face perception. *Trends Cogn Sci, 4*(6), 223-233.

Haxby, J. V., Hoffman, E. A., & Gobbini, M. I. (2002). Human neural systems for face recognition and social communication. [Review]. *Biol Psychiatry, 51*(1), 59-67.

Herrington, J. D., Taylor, J. M., Grupe, D. W., Curby, K. M., & Schultz, R. T. (2011). Bidirectional communication between amygdala and fusiform gyrus during facial recognition. [Research Support, N.I.H., Extramural]. *Neuroimage, 56*(4), 2348-2355. doi: 10.1016/j.neuroimage.2011.03.072

Holland, D., Kuperman, J. M., & Dale, A. M. (2010). Efficient correction of inhomogeneous static magnetic field-induced distortion in Echo Planar Imaging. [Research Support, N.I.H., Extramural]. *Neuroimage, 50*(1), 175-183. doi: 10.1016/j.neuroimage.2009.11.044

Laeng, B., Profeti, I., Saether, L., Adolfsdottir, S., Lundervold, A. J., Vangberg, T., . . . Waterloo, K. (2010). Invisible expressions evoke core impressions. *Emotion, 10*(4), 573-586. doi: 10.1037/a0018689

LeDoux, J. E. (1996). *The emotional brain: The mysterious underpinnings of emotional life. .* New York, NY: Simon & Schuster.

Li, J., Liu, J., Liang, J., Zhang, H., Zhao, J., Rieth, C. A., . . . Lee, K. (2010). Effective connectivities of cortical regions for top-down face processing: a dynamic causal modeling study. [Research Support, N.I.H., Extramural

Research Support, Non-U.S. Gov't

Research Support, U.S. Gov't, Non-P.H.S.]. *Brain Res, 1340*, 40-51. doi: 10.1016/j.brainres.2010.04.044

Lundqvist, D., Flykt, A., & Öhman, A. (1998). *The Karolinska Directed Emotional Faces - KDEF, CD ROM*.

Maldjian, J. A., Laurienti, P. J., Kraft, R. A., & Burdette, J. H. (2003). An automated method for neuroanatomic and cytoarchitectonic atlas-based interrogation of fMRI data sets. *Neuroimage, 19*(3), 1233-1239.

Penny, W. D., Stephan, K. E., Daunizeau, J., Rosa, M. J., Friston, K. J., Schofield, T. M., & Leff, A. P. (2010). Comparing Families of Dynamic Causal Models. *Plos Computational Biology, 6*(3). doi: ARTN e1000709

DOI 10.1371/journal.pcbi.1000709

Penny, W. D., Stephan, K. E., Mechelli, A., & Friston, K. J. (2004). Comparing dynamic causal models. [Comparative Study]. *Neuroimage, 22*(3), 1157-1172. doi: 10.1016/j.neuroimage.2004.03.026

Perrett, D., & Mistlin, A. J. (1990). Perception of facial characteristics by monkeys. *Comparative Perception, 2*, 187-215.

Perrett, D. I., Hietanen, J. K., Oram, M. W., & Benson, P. J. (1992). Organization and functions of cells responsive to faces in the temporal cortex. [Research Support, Non-U.S. Gov't]. *Philos Trans R Soc Lond B Biol Sci, 335*(1273), 23-30. doi: 10.1098/rstb.1992.0003

Pitcher, D., Garrido, L., Walsh, V., & Duchaine, B. C. (2008). Transcranial magnetic stimulation disrupts the perception and embodiment of facial expressions. [Research Support, Non-U.S. Gov't]. *J Neurosci, 28*(36), 8929-8933. doi: 10.1523/JNEUROSCI.1450-08.2008

Pitcher, D., Walsh, V., Yovel, G., & Duchaine, B. (2007). TMS evidence for the involvement of the right occipital face area in early face processing. [Research Support, Non-U.S. Gov't]. *Current Biology, 17*(18), 1568-1573. doi: 10.1016/j.cub.2007.07.063

Puce, A., & Perrett, D. (2003). Electrophysiology and brain imaging of biological motion. [Research Support, Non-U.S. Gov't

Review]. *Philos Trans R Soc Lond B Biol Sci, 358*(1431), 435-445. doi: 10.1098/rstb.2002.1221

Raftery, A. E. (1995). Bayesian model selection in social research. *Sociological Methodology 1995, Vol 25, 25*, 111-163.

Stephan, K. E., Penny, W. D., Daunizeau, J., Moran, R. J., & Friston, K. J. (2009). Bayesian model selection for group studies. [Research Support, Non-U.S. Gov't]. *Neuroimage, 46*(4), 1004-1017. doi: 10.1016/j.neuroimage.2009.03.025

Turk-Browne, N. B., Norman-Haignere, S. V., & McCarthy, G. (2010). Face-Specific Resting Functional Connectivity between the Fusiform Gyrus and Posterior Superior Temporal Sulcus. *Front Hum Neurosci, 4*, 176. doi: 10.3389/fnhum.2010.00176

Vuilleumier, P., Armony, J. L., Driver, J., & Dolan, R. J. (2003). Distinct spatial frequency sensitivities for processing faces and emotional expressions. *Nat Neurosci, 6*(6), 624-631. doi: Doi 10.1038/Nn1057

Vytal, K., & Hamann, S. (2010). Neuroimaging support for discrete neural correlates of basic emotions: a voxel-based meta-analysis. [Meta-Analysis]. *J Cogn Neurosci, 22*(12), 2864-2885. doi: 10.1162/jocn.2009.21366

Williams, L. M., Das, P., Liddell, B. J., Kemp, A. H., Rennie, C. J., & Gordon, E. (2006). Mode of functional connectivity in amygdala pathways dissociates level of awareness for signals of fear. [Randomized Controlled Trial

Research Support, Non-U.S. Gov't]. *J Neurosci, 26*(36), 9264-9271. doi: 10.1523/JNEUROSCI.1016-06.2006

Winston, J. S., Strange, B. A., O'Doherty, J., & Dolan, R. J. (2001). Automatic and intentional brain responses during evaluation of trustworthiness of faces. *Nat Neurosci, 5*(3), 277-283.

Winston, J. S., Vuilleumier, P., & Dolan, R. J. (2003). Effects of low-spatial frequency components of fearful faces on fusiform cortex activity. *Current Biology, 13*(20), 1824-1829. doi: Doi 10.1016/J.Cub.2003.09.038

Wojciulik, E., Kanwisher, N., & Driver, J. (1998). Covert visual attention modulates face-specific activity in the human fusiform gyrus: fMRI study. [Research Support, Non-U.S. Gov't

Research Support, U.S. Gov't, P.H.S.]. *Journal of Neurophysiology, 79*(3), 1574-1578.